NbTiN BASED TUNING STRUCTURES FOR BROADBAND Nb-Al$_2$O$_3$-Nb SIS MIXERS FROM 640 GHz– 800 GHz

S. Glenz, S. Haas, C.E. Honingh, K. Jacobs

KOSMA, I. Physikalisches Institut, Universität zu Köln
Zülpicher Strasse 77, 50937 Köln, Germany

We present measurements with a prototype waveguide SIS mixer for band 2 (640 GHz – 800 GHz) of HIFI (Heterodyne Instrument for FIRST). The Nb/Al$_2$O$_3$/Nb junctions have an R$_n$A product from 12–18 $\Omega\mu$m^2. These junctions are embedded in microstrip circuits tuning out the device capacitance using a NbTiN ground layer and various top conductor materials such as NbTiN, Nb and Al. The NbTiN films are fabricated by DC magnetron sputtering which is optimized for a minimum value of the DC resistivity and for a high critical temperature by varying the sputter pressure, sputter power and Ar:N$_2$ flow. Typical NbTiN film parameters for device fabrication are ρ = 120 $\mu\Omega$cm and T$_c$ = 14.5 K. The best uncorrected noise temperatures we measured so far are for devices with NbTiN/SiO$_2$/Nb tuning. At 4.2 K bath temperature, a standard Y-factor measurement yields uncorrected receiver noise temperatures of 350 K at 642 GHz and 500 K at 810 GHz for 1.5 GHz intermediate frequency. We discuss the effect of the various tuning circuit materials on the mixer performance. In addition, measurements at IF's between 4 GHz and 8 GHz will be presented.

1. INTRODUCTION

Our aim is to develop an SIS mixer for Band 2 of the HIFI instrument for the Herschel Space Observatory (formerly known as FIRST) [1]. The specifications for this instrument require a broadband and low noise receiver channel which covers frequencies from 640 GHz to 800 GHz. State-of-the-art mixers implementing Nb/Al$_2$O$_3$/Nb tunnel junctions and integrated Nb tuning circuits can have quantum limited noise performance up to the gap frequency Δ/h of niobium at about 700 GHz. Above this frequency, RF loss in the niobium tuning structure increases rapidly, whereas the SIS tunnel junction itself can be used as a mixer up to 2Δ/h.

Unfortunately, the niobium gap frequency splits band 2 of HIFI, so we have to find the most suitable material or a combination of different materials to obtain the most sensitive device for the complete frequency range.

Over the last few years efforts to find a superconducting material with a higher gap than niobium, compatible to the Nb/Al$_2$O$_3$/Nb junction technology, led to the use of NbTiN films for tuning circuits [2] as well as for the junction electrodes [3].

There are also recent developments of SIS mixers with aluminum [4] or a combination of aluminum and niobium [5] for the tuning circuits that resulted an improvement in the mixer sensitivity compared to a pure Nb device.

In this paper we present DC and RF measurements of devices with NbTiN for the ground plane of the microstrip tuning circuit, SiO_2 for the dielectric, and either NbTiN, Nb, or Al as top conductor material, with integrated $Nb-Al_2O_3-Nb$ tunnel junctions.

2. NbTiN FILM FABRICATION AND CHARACTERIZATION

The NbTiN layers are fabricated by reactive DC-magnetron sputtering of NbTi in an Argon/Nitrogen atmosphere. The target (NbTi 78:22 wt.%, 3" diameter) is mounted in a AJA model 330 sputter source with an integrated gas inlet ring positioned in close vicinity of the target. A modular magnet ring allows an unbalanced magnetic field constellation to increase plasma heating of the substrate. The distance between sputter source and substrate is about 8 cm which is the maximum for the system. Tests with different heights (7 cm, 5.5 cm) did not improve the film properties. The sputter chamber is evacuated by a Cryotorr 8 pump to a base pressure $< 1 \cdot 10^{-8}$ mbar. The Ar/N_2 pressure is regulated by throttling the gate valve to the cryopump. The substrate is thermally coupled to a copper pallet which is placed on the water cooled substrate station to achieve stable and reproducible thermal conditions at moderate temperatures during film deposition. To determine the film quality, we measured the normal state resistivity and the critical temperature of NbTiN films with a thickness of 350 nm. The normal state resistivity of the film above T_c (20 K) is taken as an indication of low RF loss, as this loss is difficult to determine directly.

The DC properties of the NbTiN films are measured in a dipstick system for measurements in liquid helium at 4.2 K, where the sample temperature is controlled by the dipstick height above the helium level. A temperature diode is integrated at the sample mount in close thermal contact to the sample. The samples are wire bonded. Using a four point probe and lock-in amplifier technique, resistances down to 10 mΩ can be measured accurately. Both characteristic DC parameters, the critical temperature and the DC resistivity of the film depend on the sputter conditions to varying degrees. Figures 1a – 1c show data sets we measured when sampling the parameter space.

Fig. 1a shows a maximum of T_c at an Ar/N_2 ratio of 91 sccm : 8 sccm. In this regime of the flow ratio, the sputter conditions are very stable and reproducible. The critical temperature shows a strong increase when the sputter power becomes higher than 250 W and attains a maximum at 325 W (Fig. 1b) at these flows, as the N_2 consumption needed for the correct stoichiometry is related to the power. The resulting discharge voltage is around 280 V.

NbTiN films with a low DC resistivity show high compressive mechanical stress, which causes a variety of fabrication difficulties leading to be a certain tradeoff between film stress and DC resistivity. The most decisive parameter to control the resistivity of the NbTiN films is the sputter pressure (Fig. 1c). The increase of the resistivity is due to a change of the film structure [6].
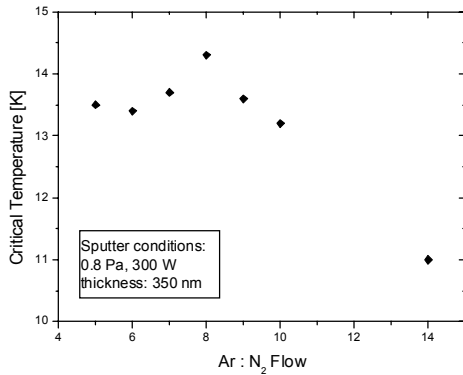
Fig. 1a   Tc versus Ar/N$_2$ flow

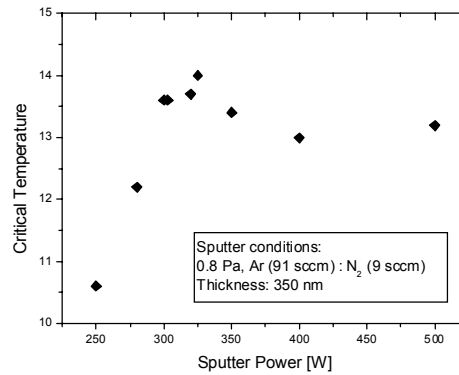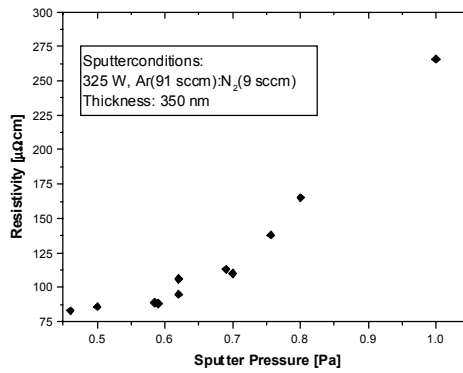
Fig. 1b Tc versus sputter power

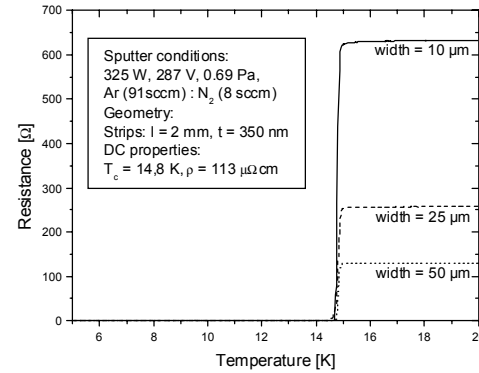Fig. 1c DC resistivity versus sputter pressure

Fig. 2: Typical R-T curves of NbTiN test structures

An example for typical NbTiN films is given in Fig. 2. It shows the R-T curves of three NbTiN strips with different width. The critical temperature is 14.8 K with a sharp transition of $\Delta T_c = 0.3$ K. The DC resistivity $\rho = 113$ µΩcm is calculated from the resistance at 20 K and the strip dimensions. These films, sputtered at ~ 0.7 Pa total pressure, exhibit a tolerable stress which still allows a successful integration of tunnel junctions.

3. MIXER DEVICE FABRICATON

In part 5 of this paper we present results. Table 1 gives an overview of three fabrication runs, which are slightly different in fabrication and use several different lithography mask sets. The main differences are the NbTiN quality, the junction barrier oxidation parameters and the deposition method for the SiO$_2$ dielectric. The results of these fabrication runs will be presented in chapter 5.

An initial stack of four layers is deposited in situ by dc magnetron sputtering on a 250 µm quartz substrate (INFRASIL). It consists a 350 nm NbTiN ground plane followed by the SIS trilayer, composed of a 100 nm Nb bottom layer followed by 8 nm Al for the tunnel

barrier and another 100 nm Nb as top electrode. The oxidation of the barrier is performed in the load-lock of the sputtering machine at a static oxygen pressure of 1.6 Pa for 7 – 8 min, resulting in a current density of j_c = 10–13 kA/cm^2. All four layers are deposited into a bilayer AZ7212 (Clariant) photoresist window with a large undercut profile. This technique [7] permits a clean liftoff process for more than 400 nm layer thickness.

For the junction definition we use standard 300 nm UV lithography with AZ7212. Minimum junction areas of 0.4 – 0.5 µm^2 can be achieved. For smaller junction areas and/or more accurate control of the junction area we will have to change this process to e-beam lithography [8].

A mixture of 6 sccm CCl_2F_2 + 1.2 sccm NF_3 is used for anisotropic reactive ion etching of the 100 nm top Niobium for 1:30 at 0.17 W/cm^2, (-105 V) and 40 µbar [5]. The Al_2O_3-Al barrier is sputter etched with 8 sccm Argon at 10 µbar and 1.1 W/cm^2 (-605 V) for 9 min. To avoid excessive heating of the photoresist and the junction barrier, we etch in 9 intervals of 1 min with 1 min cooling breaks. The Nb bottom electrode is etched again with CCl_2F_2 + NF_3. As a dielectric layer for the RF tuning circuit and for junction insulation we use SiO_2 with a thickness of 230 nm, deposited either by e-beam evaporation or RF sputtering and defined in the usual self-aligned liftoff procedure. The 350 nm thick top wiring layer is DC-magnetron sputtered and defined by a subsequent liftoff. We produced and studied devices with either NbTiN, Al, or Nb top wiring layers, with some wafers having two different wiring material layers which were sputtered sequentially with the other part of the wafer covered by photoresist. The devices with aluminum top wiring are covered with 70 nm Niobium to eliminate the DC series resistance and are passivated with 300 nm SiO_2 to protect the aluminum from chemical attack.
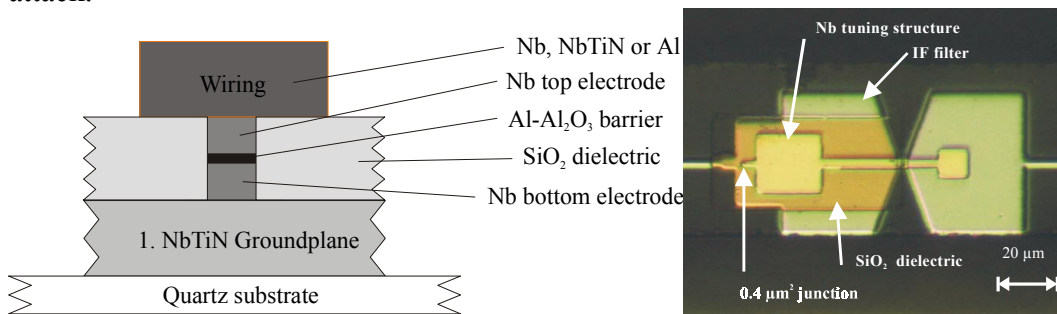

Fig. 3 Sketch of the layer sequence of junction and tuning structure   Fig. 4 Microscope photo of a finished device

The fabricated devices have areas of 0.4 µm^2 and 0.6 µm^2. Fig. 4 shows a top view of a finished device after dicing and thinning. The tuning circuit is an end loaded stub followed by two Tchebychev transformer sections. All tested devices are designed for HIFI Band 2 (640-800 GHz). The design is optimized for band flatness with an calculated coupling of 60-70 % over the whole band. For the top wiring we used NbTiN, Nb or Al. Niobium has the advantage to be lossless up to the gap Δ/h = 700 GHz, but above the loss rises rapidly which complicates the flat band design. Aluminum is a normal conductor at 4.2 K with only a small variation in conductivity over the band. This helps achieving a broad bandwidth but has a penalty in noise performance especially at the low end of

band. Having both wiring electrodes made of NbTiN leads to DC and RF heating effects [9].

Table 1: Differences in fabrication between the batches A. B and C

Batch #	Ground layer	Ground plane ρ / T_c	Oxidation time / pressure	Dielectric SiO_2 deposition
A	350 nm NbTiN	134 μΩcm 14.3 K	8:00 1.6 Pa	Evaporated 400 W
B	280 nm NbTiN	125 μΩcm 14.4 K	8:10 1.56 Pa	RF sputtered 1 Pa, 300 W
C	350 nm NbTiN	100 μΩcm 15.1 K	7:00 1.6 Pa	RF sputtered 1 Pa, 300 W

4. DC MEASUREMENTS

After the fabrication the current-voltage characteristics of the devices were DC tested in a dipstick system at 4.2 K which allows the determination of the $R_N A$ product. The voltage of the self induced step resonance of the integrated tuning circuit gives a first indication about the RF performance of the device.
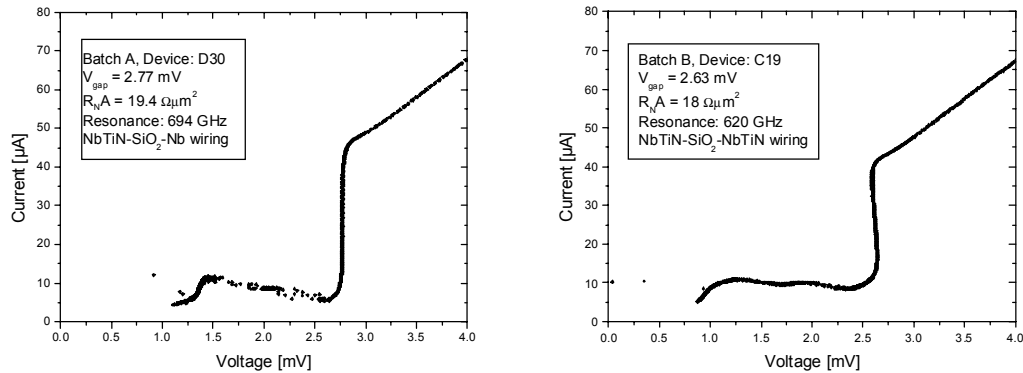

Fig. 5: IV characteristic of a Nb/Al$_2$O$_3$/Nb junction with:

5a: NbTiN/SiO$_2$/Nb tuning   5b: NbTiN/SiO$_2$/NbTiN tuning

The IV-curves in Fig. 5a and b are measured with a dipstick at 4.2 K. Fig. 5a shows a typical IV-curve for a SIS mixer with a hybrid NbTiN/SiO$_2$/Nb tuning circuit is shown. The gap voltage is 2.77 mV. The $R_{sg}(2mV)/R_N$ ratio is determined from the I/V-curves with magnetic field in Fig. 6 (R_{sg}/R_N = 7.4 for device A D30). A resonant mode of the integrated tuning circuit shows up as a current peak at 1.43 mV, corresponding to a Josephson oscillation frequency of 694 GHz. The device in Fig. 5b employs a NbTiN/SiO$_2$/NbTiN tuning circuit and shows backbending at the gap as well as an obvious gap voltage depression (V_{gap} = 2.65 mV). Both effects can be explained by heat trapping in the junction [9].
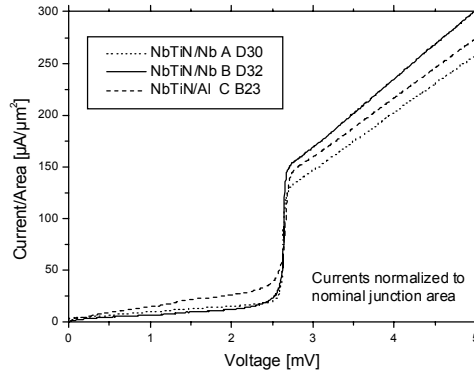
Fig. 6 Comparison between the unpumped IV curves
scaled to the nominal junction areas of different batches

The currents shown in Fig. 6 are normalized to the nominal junction mask size. The self induced resonances are suppressed by a magnetic field. Differences in the current rise at the gap and the subgap current give an indication about the junction quality. The variation in the gap current rise of the devices is mainly due to size variations, which can be as high as 20-30% for device areas of 0.5 μm^2 fabricated by UV lithography. The devices from the batches A and B are of similar quality and their R_{sg}/R_N ratio is 7.4 (Device D30) and 10.9 (Device D32), respectively. The leakage rate of batch C with $R_{sg}/R_N = 4.33$ (Device B23) is noticeably higher than for the batches A and B and leads to a higher noise temperature of the device. A calculation using the quantum mixer theory [10] shows that the increase in noise temperature can be expected to be between 150-200 K. Table 2 gives an overview of the DC properties of the devices. RF measurements are presented in the next section.

Table 2: DC characteristics of devices from 3 batches

Batch/device	Top wiring Material	Nominal junction area:	R_N	R_{sg}/R_N
A / E17	Nb	0.36 μm^2	49 Ω	8.5
A / D30	Nb	0.36 μm^2	54 Ω	7.4
B / D32	Nb	0.36 μm^2	44 Ω	10.9
B / C19	NbTiN	0.36 μm^2	59 Ω	8.5*
C / B23	Al	0.64 μm^2	29 Ω	4.33
C / B17	Al	0.64 μm^2	22 Ω	4.2
C / D27	Nb	0.64 μm^2	29 Ω	4.3

* The subgap current of device B C19 is noticeably higher than for other devices from this batch with Nb top wiring. This is supposed to be due to the higher temperature of the tunnel junction embedded in the NbTiN wiring which enhances the subgap current and reduces the R_{sg}/R_N ratio.

5. RF MEASUREMENTS

The receiver setup is described in detail in [11]. To verify the response of the junction over the band we use a Fourier Transform Spectrometer to measure the direct detection of the device. The optical path of the FTS beam is evacuated.

The solid state local oscillators have frequency ranges from 630-690 GHz and 780-820 GHz. The LO power and the hot (295 K) / cold (77 K) signal are injected via a 36 μm Mylar beamsplitter, a 500 μm teflon dewar window at 295 K and a 300 μm teflon IR filter at 77 K to the antenna horn of the fixed tuned waveguide (330x90 μm^2) mixer. Using the standard Y-factor method we calculate the uncorrected noise temperature of the receiver.

The IF output signal is connected to a HEMT amplifier on the 4 K stage and further amplified with an IF chain at 295 K by about 70 dB. In our standard setup we use a 1-2 GHz HEMT amplifier [12] and a bandpass filter restricting the IF bandwidth to 100 MHz at 1.4 GHz center frequency. No isolator or matching circuit is used. A second HEMT amplifier [13] is used for IF measurements from 4-8 GHz. The 4-8 IF mixer output signal is coupled to the HEMT amplifier with a 4-8 GHz Pamtech isolator between mixer and amplifier. Both amplifiers have comparable noise temperatures ($T_{IF} = 4$-8 K).

Fig. 7 shows the trend of the measured receiver noise temperatures as a function of local oscillator frequency for devices from all three batches and with NbTiN, Nb or Al as top wiring layer. All devices are measured at 4.2 K bath temperature with the 1-2 GHz HEMT amplifier. For all measurements (except for the device A E17) a corrugated feedhorn with its center frequency at 675 GHz is used For device A E17 we used a Potter-horn optimized for 800 GHz.
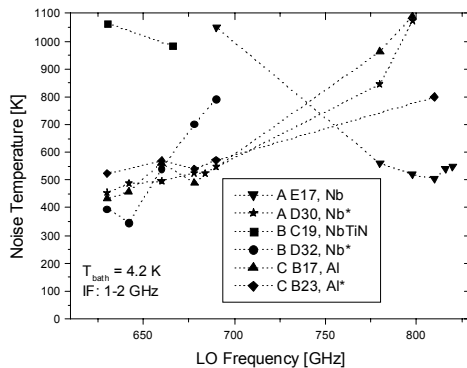

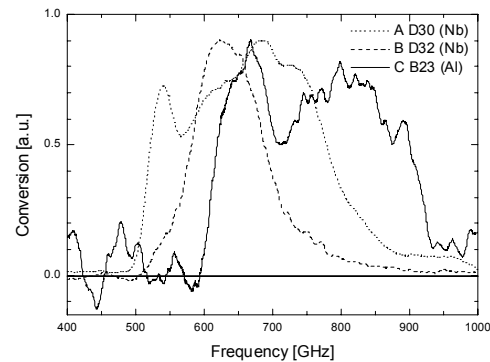Fig. 7: Overview: Noise Temperatures of devices with different top wiring layers

Fig. 8: FTS traces of three devices

The best uncorrected noise temperatures are 350 K at 642 GHz for device B D32 and 500 K at 800 GHz for device A E17. Both devices have a Nb top wiring layer. The noise temperature of the one device with a NbTiN top layer is about a factor of 2 higher than of the devices with Al and Nb. There are devices with Nb (A D30) as well as with Al (C B23) top wiring layer that show broadband response from 640-800 GHz.

This corresponds to the FTS measurements shown in Fig. 8. Both curves are normalized to their peak values. The FTS traces of the devices A D30 with Nb top wiring and C B23 with Al top wiring show a broadband coupling of at least 160 GHz in width but it is obviously difficult to position the band center at exactly 720 GHz. The shift of the band is mainly due to variations in the junction area but also due to resistivity variations of the NbTiN ground layer. The bandwidth of device B D32 is noticeably smaller. We attribute this to the insufficient thickness of the NbTiN ground plane, which is close to or less than one penetration depth.
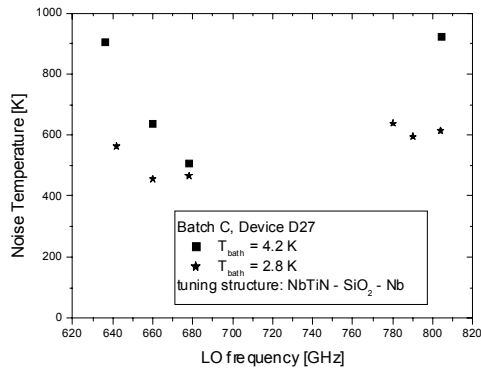

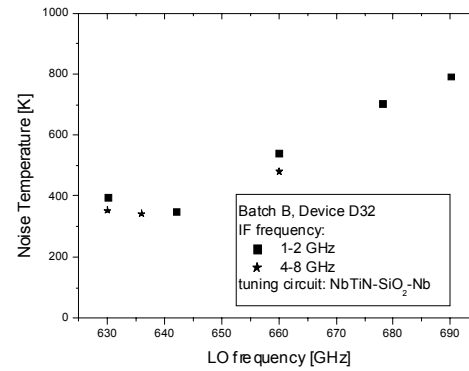Fig. 9 Results at 2.8 K bath temperature   Fig. 10 Results with different IF frequencies

The effect of decreasing the bath temperature from 4.2 K to 2.8. K is shown in Fig. 9 for a device with Nb top wiring layer. The significant improvement in the noise temperature on the upper band side is due to an increase of the Nb gap. The unexpected decrease of the noise temperature at the lower band end can be explained by the strong variation of the phase velocity in the microstrip caused by temperature dependence of the Nb top electrode material. In the present design, this seems results in a shift of the lower band edge to lower frequencies.

The IF band for the HIFI instrument is specified to be 4-8 GHz. Fig. 10 shows a comparison of the noise temperatures of device C D27 measured with both the 1-2 GHz HEMT amplifier and the 4-8 GHz HEMT amplifier. The resulting receiver noise temperatures for both devices are comparable at 4.2 K. The noise temperature with the 4-8 GHz amplifier is measured including the full 4 GHz IF bandwidth while a 100 MHz bandpass filter with 1.4 GHz center frequency was used for the 1-2 GHz IF data.

6. SUMMARY

We developed a deposition process for NbTiN films by using DC reactive magnetron sputtering. The films are optimized for a low DC resistivity and a high critical temperature and high reproducibility. We have shown that films with a resistivity of $\rho = 100\text{-}140\ \mu\Omega\text{cm}$ and a critical temperature $T_c = 14\text{-}15$ K can be successfully integrated in a junction fabrication process.

We fabricated and tested Nb-Al$_2$O$_3$-Nb tunnel junctions embedded in wiring structures with a NbTiN ground plane, a SiO$_2$ dielectric and NbTiN, Al, or Nb for the top wiring layer. The quality of the devices varies from is varying from R$_{sg}$/R$_N$ = 4.5 to R$_{sg}$/R$_N$ = 9. The devices are fabricated for the HIFI instrument which requires a fractional bandwidth of 22 %. The FTS results show that we are able to achieve the bandwidth but it is difficult to position the band center, mostly due to the large junction area variation due to the optical lithography of 0.36 µm^2 to 0.64 µm^2 devices. This can be improved by using electron beam lithography.

Based on the heterodyne noise measurements and FTS results there is no clear preference of a tuning circuit top electrode material yet. This decision is complicated by the fact that the DC IV-curves of batch C, which is the first batch with Al devices, have a higher leakage rate which increase the measured noise temperatures.

ACKNOWLEDGMENT

REFERENCES

[1] http://saturn.sron.nl/hifi/

[2] J. W. Kooi, J. A. Stern, G. Chattopadhyay, H. G. LeDuc, B. Bumble, J. Zmuidzinas, "Low-loss NbTiN films for THz SIS mixer tuning circuits", Proc. of 8th Int. Symp. on Space Terahertz Techn. 1997, pp. 310-319

[3] B. Bumble, H. G. LeDuc, J. A. Stern, "Fabrication of Nb/Al-N$_x$/NbTiN junctions for SIS mixer applications above 1 THz", Proc. of 9th Int. Symp. on Space Terahertz Techn. 1998, pp. 295-304

[4] M. Bin, M. C. Gaidis, J. Zmuidzinas, T. G. Phillips, H. G. LeDuc, "Low noise 1 THz niobium superconducting tunnel junction mixer with normal metal tuning circuit", Appl. Phys. Lett., vol. 68, pp. 1714-1716, 1996

[5] S. Haas, S. Wulff, D. Hottgenroth, C.E. Honingh, K. Jacobs, " Broadband Array SIS Mixers for 780-880 GHz with Aluminium tuning circuit", Proc. of 11. Int. Symp. on Space Terahertz Technol. 2000, pp. 95-104

[6] N. N. Iosad, A. V. Mijrishii, V. V. Roddatis, N. M. van der Pers, B. D. Jackson, J. R. Gao, S. N. Polyakov, P. N. Dimitriev, T. M. Klapwijk, "Properties of (Nb, Ti)N thin films deposited on silicon wafers at ambient substrate temperatures", J. of Appl. Phys. vol. 88, issue 10, pp. 5756-5759, 2000

[7] G. J. Dolan, "Offset masks for lift-off photoprocessing", Appl. Phys. Lett. vol. 31 no. 5, pp.337-339, 1977

[8] P. Puetz, K. Jacobs, "E-Beam SIS junction fabrication using CMP and E-Beam defined wiring layer", Proc. of the Tenth Int. Symp. on Space Terahertz Techn. 1999, pp. 118-129

[9] B. Leone, B. D. Jackson, J. R. Gao, T. M. Klapwijk, "Geometric heat trapping in niobium superconductor-insulator-superconductor mixers due to niobium titanium nitride leads", Appl. Phys. Lett. 76, 780-782, 2000

[10] J. R. Tucker, M. J. Feldmann, "Quantum detection at millimeter wavelength", Rev. Mod. Phys., vol. 57, no. 4, 1885

[11] S. Haas, C. E. Honingh, D. Hottgenroth, K. Jacobs, J. Stutzki, "Low noise tunerless waveguide SIS receivers for 440-500 GHz and 630-690 GHz", Int. J. Infrared Millimeter Waves, 17, 1996, pp. 493-506

[12] B. Vowinkel, Ph. Müller, "Cryogenic L-band HEMT-amplifier with a noise figure of less than 0.1 dB", Proc. 5th Microwave and Optronics Conf., Stuttgart, 1990

[13] Yebes: http://www.oan.es/cay/index.shtml.en